Dynamin Is Membrane-Active: Lipid Insertion Is Induced by Phosphoinositides and Phosphatidic Acid[†]

Koert N. J. Burger,*,‡,§ Rudy A. Demel,‡ Sandra L. Schmid,‖ and Ben de Kruijff‡

Department of Biochemistry of Membranes, Centre for Biomembranes and Lipid Enzymology, Institute of Biomembranes, Utrecht University, Padualaan 8, 3584 CH Utrecht, The Netherlands, and Department of Cell Biology, The Scripps Research Institute, 10550 North Torrey Pines Road, La Jolla, California 92037

ABSTRACT: Dynamin is a large GTPase involved in the regulation of membrane constriction and fission during receptor-mediated endocytosis. Dynamin contains a pleckstrin-homology domain which is essential for endocytosis and which binds to anionic phospholipids. Here, we show for the first time that dynamin is a membrane-active molecule capable of penetrating into the acyl chain region of membrane lipids. Lipid penetration is strongly stimulated by phosphatidic acid (PA), phosphatidylinositol 4-phosphate, and phosphatidylinositol 4,5-bisphosphate. Though binding is more efficient in the presence of the phosphoinositides, a much larger part of the dynamin molecule penetrates into PA-containing mixed-lipid systems. Thus, local lipid metabolism will dramatically influence dynamin−lipid interactions, and dynamin−lipid interactions are likely to play an important role in dynamin-dependent endocytosis. Our data suggest that dynamin is directly involved in membrane destabilization, a prerequisite to membrane fission.

Dynamin plays an essential role at the plasma membrane in receptor-mediated endocytosis and synaptic vesicle recycling (*1*). The importance of dynamin in endocytosis became evident when the product of the *shibire* gene in *Drosophila* was found to be homologous to dynamin. Flies expressing a temperature-sensitive mutant of the *shibire* gene product have a paralytic phenotype at the nonpermissive temperature. Morphologically, this results in an accumulation of endocytic pits at the presynaptic membrane, many of which have an electron-dense band or 'collar' around their necks (*2*, *3*). Long tubular membranes decorated with dynamin spirals and often capped with a clathrin-coated bud also accumulate in isolated nerve terminals treated with GTPγS (*4*). Finally, overexpression of a mutant dynamin deficient in GTP binding blocks endocytosis in transfected mammalian cells (*5*, *6*). Together these data suggest a model in which oligomerization of dynamin induces membrane constriction and the pinching-off of endocytic vesicles, driven by a conformational change of dynamin upon GTP hydrolysis (*1*, *7*).

This *pinchase-model* of dynamin function is supported by in vitro experiments using isolated dynamin. Dynamin, present in the cytosol as a homotetramer (*8*), self-assembles into rings and spirals upon dilution in buffers of low ionic strength (*9*). GTP destabilizes these supramolecular complexes of dynamin (*10*). In addition, dynamin transforms liposomes containing anionic phospholipids into dynamin-coated tubules with a morphology very similar to that found in GTPγS-treated nerve terminals. Depending on their lipid composition, these tubules vesiculate upon addition of GTP (*7*, *11*, *12*). Finally, the GTPase activity of dynamin in vitro is greatly increased by self-association, in particular when this occurs on acidic phospholipid-containing membrane tubules, suggesting that GTPase activation is required for the pinchase action of dynamin. Dynamin contains a number of distinct functional domains, an N-terminal GTPase domain, a pleckstrin-homology (PH)[1] domain, a proline- and arginine-rich domain (PRD), and a GTPase effector domain (GED). Mutations in GED result in a loss of assembly-stimulated GTPase activity of dynamin in vitro but, unexpectedly, stimulate endocytosis in cells transiently overexpressing the dynamin mutants (*13*). These in vivo data suggest that dynamin does not act as a mechanochemical enzyme driving membrane fission, but instead, like other members of the GTPase superfamily, functions as a molecular switch regulating downstream effectors of membrane fission (*molecular switch model*). However, though the in vivo data argue against assembly-stimulated GTP hydrolysis providing the driving force for membrane fission, it remains possible that other activities of dynamin are directly required for membrane bending or fission.

In all current models of dynamin-mediated endocytosis, dynamin intimately interacts with the membrane at the neck

---

* To whom correspondence should be addressed. Fax +31-30-251 3655, phone +31-30-253 2885 or 3313, e-mail K.N.J.Burger@bio.uu.nl.

‡ Utrecht University.

§ Present address: Department of Molecular Cell Biology, Institute of Biomembranes, Utrecht University, Padualaan 8, 3584 CH Utrecht, The Netherlands.

‖ The Scripps Research Institute.

[1] Abbreviations: Chol, cholesterol; GED, GTPase effector domain; LPA, lyso-PA; PA, phosphatidic acid; PC, phosphatidylcholine; PE, phosphatidylethanolamine; PH, pleckstrin-homology; PLC-δ, phospholipase-Cδ; PRD, proline-rich domain; PS, phosphatidylserine; PtdIns, phosphatidylinositol; PtdIns-4-P, PtdIns-4-phosphate; PtdIns-4,5-P_2, PtdIns-4,5-bisphosphate.

of a deeply invaginated coated pit. The aim of the present study is to determine whether, during its interaction with the membrane, dynamin is able to penetrate into the cytosolic leaflet of the membrane. Membrane penetration would stably anchor the membrane fission machinery at its proper location, and could even play a direct role in the induction of membrane curvature, or in membrane destabilization and fission. To this end, we characterized the interaction of dynamin with lipid monolayers spread at the air−water interface and determined its lipid specificity. Lipid monolayers, when used at sufficiently high surface pressures, faithfully mimic the lipid packing properties of biomembranes, and are a reliable model system to study the mechanism by which membrane-active proteins insert into cell membranes (reviewed in *14*, *15*). Monolayer systems are unique in that they allow direct and kinetic data to be obtained on protein−lipid binding as well as protein−lipid insertion using only very small amounts of material (1−2 nmol of lipid and 1−20 μg of protein).

Our data show that dynamin binds to anionic phospholipids. In addition, we demonstrate for the first time that, as a result of this interaction, dynamin inserts into the lipid layer. Dynamin's membrane activity is strongly enhanced by phosphoinositides and in particular by PA. We discuss these results in light of recent findings on the role of phosphoinositides and PA in endocytosis (*16−18*), and propose a new model for dynamin function in which a local change in lipid composition results in deep penetration of dynamin into the membrane, membrane destabilization, and fission.

MATERIALS AND METHODS

Materials. Bovine brain PtdIns-4-phosphate (PtdIns-4-P) and PtdIns-4,5-bisphosphate (PtdIns-4,5-P$_2$) were obtained from Boehringer (Mannheim, FRG). A brain total lipid extract (type VII), a brain lipid extract enriched in phosphoinositides, and bovine brain non-hydroxy fatty acid galactosylceramide were obtained from Sigma Chemical Co. (St. Louis, MO), and cholesterol (Chol) was from Merck (Darmstadt, FRG). Plant PtdIns and the (1,2-dioleoyl) phospholipids, PC, PE, PS, and PA, were from Avanti Polar Lipids, Inc. (Birmingham, AL). GTP and GTPγS were from Sigma Chemical Co., and [^{14}C]formaldehyde was from NEN Life Science Products, Inc. (Boston, MA). Phospholipids were >95% pure as judged by high-performance thin-layer chromatography. All other reagents and chemicals were of analytical grade.

Proteins. Human recombinant dynamin-1 and the ΔPRD−dynamin construct were expressed in Tn5 cells using a baculovirus expression system, purified as described (*8*, *10*), and stored at −80 °C in 0.5 M potassium phosphate (pH 7.0). The ΔPRD−dynamin construct contains a stop codon at amino acid residue 751 of the hemagglutinin-tagged wild-type dynamin-1 sequence. Proteins were dialyzed overnight against 20 mM Hepes−NaOH (pH 7.0), 1 mM MgCl$_2$, 2 mM EGTA, 150 mM NaCl, and 1 mM DTT (HCB150), and subjected to low-speed centrifugation to remove possible aggregates (Eppendorf microfuge, 5 min, 8000 rpm). Aliquots of the supernatant were stored at −80 °C and used within 2 months. After rapid thawing, they were diluted 10-fold in monolayer buffer (see below), and any aggregates were removed (as above). The dynamin-1, dynamin-2, and the PLC-δ (wild-type and mutant) PH domains were

produced as soluble proteins in *Escherichia coli*, purified as described (*19−21*), and stored at −80 °C in Mes−glycerol buffer (25 mM Mes, pH 6.8, 1 mM DTT, 10% glycerol, and 100 mM NaCl). No detergents were used during protein purification. All proteins were over 95% pure as judged by overloaded Coomassie-blue-stained SDS−PAGE. For binding experiments, dynamin-1 and the PH domain of dynamin-1 were ^{14}C-labeled using mild reductive methylation of the α- and ε-amino groups (*22*). In short, dynamin-1 (8 nmol) was incubated with [^{14}C]formaldehyde (240 nmol; 53 Ci/mol) and NaCNBH$_3$ (25 mM) in 250 mM potassium phosphate (pH 7.0) for 1 h at 20 °C under constant stirring, and nonreacted label was removed using a Sephadex G50 spin-column. Over 98.5% of the radioactivity ended up in the protein pellet after TCA precipitation, indicating that the [^{14}C]dynamin contained virtually no free label. [^{14}C]Dynamin was stored at −80 °C in HCB150, and the specific activity was 1007 dpm/pmol, i.e., on average, 8.6 methylated amino groups per dynamin monomer. The PH domain of dynamin-1 was labeled after exchanging the Mes−glycerol buffer for 50 mM potassium phosphate buffer (pH 7.0) using a Sephadex G25 spin-column. A 5-fold molar excess of [^{14}C]-formaldehyde was used, resulting in a specific activity of 50.3 dpm/pmol, on average, 0.4 methylated amino group per molecule. [^{14}C]-PH was stored at −80 °C in Mes−glycerol buffer. Before use, all proteins were diluted at least 10-fold in monolayer buffer. Protein concentrations were determined with BSA as a standard (*23*).

Monolayer Measurements. Stock solutions of lipids were prepared in chloroform/methanol (1:1, v/v). The phospholipid phosphorus concentration was determined using the method of (*24*). The final lipid mixtures were made at a concentration of approximately 200 μM in chloroform with 10−30% methanol and, in the case of polyphosphoinositide-containing stocks, up to 2% water. A lipid monolayer was spread at the air−water interface, and the surface pressure of the monolayer was measured by the Wilhelmy-plate method, using a Cahn 2000 electrobalance (reviewed in *14*). Experiments were performed in a thermostatically controlled cabinet flushed with nitrogen gas, in a humidified atmosphere at 37 °C (unless stated otherwise). The subphase contained 20 mM Hepes−NaOH (pH 7.0), 1 mM MgCl$_2$, 2 mM EGTA, 100 mM NaCl, and 1 mM DTT (HCB100), and was continuously stirred with a magnetic bar. Proteins were injected through a small hole at the side of the monolayer trough; the injection volume was less than 1% of the volume of the subphase. For nonradioactive experiments, and off-line radioactive experiments, at constant area, a 1.6 mL Teflon trough, 2 cm in diameter with a monolayer surface area of 3.14 cm^2, and a Wilhelmy plate with a length of 0.98 cm were used. The radioactivity in the monolayer was determined by liquid scintillation counting after flushing the trough with 10 volumes of buffer (11 min, 1.5 mL/min), collecting the monolayer quantitatively together with ∼0.5 mL of subphase, and correcting for residual radioactivity in the subphase (<30 dpm or 0.03 pmol of [^{14}C]dynamin in 0.5 mL of subphase). Monolayers were collected after the surface pressure had reached equilibrium, 30−35 min after dynamin addition. On-line radioactive experiments were performed at constant area using a 19 mL Teflon trough of ∼5.1 × 5.9 cm (monolayer area of 30.2 cm^2). Surface radioactivity was measured using a gas flow counter. The surface radioactivity is an excellent
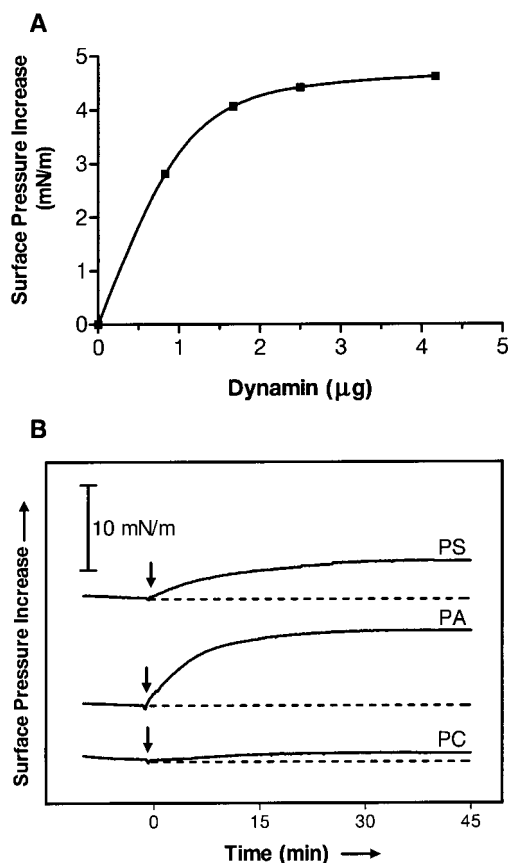
FIGURE 1: Membrane activity of dynamin. Insertion of dynamin into lipid monolayers spread at an initial surface pressure of 25 mN/m. (A) Monolayer surface pressure increase as a function of the amount of dynamin injected into the subphase (1.6 mL) underneath a single-lipid monolayer composed of PS. (B) Surface pressure increase as a function of lipid composition; the arrow indicates injection of 2.5 μg of dynamin-1 ($\sim$25 pmol) into single-lipid monolayers composed of PS, PA, or PC. Constant area experiments (monolayer area of 3.14 cm^2) at 37 °C.

measure of the radioactivity of the monolayer, because the ^{14}C-label is almost completely quenched in the subphase (*25*). After the surface pressure reached equilibrium, the trough was flushed with 10 volumes of buffer (38 min, 4.9 mL/min), and the monolayer radioactivity was determined both on-line and off-line. For measurements at constant surface pressure, a Teflon trough with three interconnected compartments of 4.3 × 4.5 cm (10 mL, surface area of 19.35 cm^2) was used at 20 °C. A lipid monolayer was spread, and proteins were injected in the first compartment and the surface area increase required for maintenance of a constant surface pressure was measured using a computer-controlled movable Teflon barrier.

RESULTS

Membrane Activity of Dynamin. To determine whether dynamin is a membrane-active molecule, a monolayer of dioleoylphosphatidylserine (PS) was spread at the air−water interface at an initial surface pressure of 25 mN/m, and increasing amounts of dynamin were injected into the subphase (Figure 1A). Dynamin induced a clear increase in surface pressure of the monolayer. This surface pressure increase was not due to the surface properties of dynamin itself, because the maximal surface pressure obtained after injecting a large excess of dynamin (12.5 μg in 1.6 mL of

subphase) in the absence of a lipid monolayer was 20.2 mN/m (not shown), i.e., much lower than the initial surface pressure of the lipid monolayer. Thus, the dynamin-induced surface pressure increase must be the result of penetration of dynamin into the lipid monolayer. A maximal increase in surface pressure was observed upon injecting 2.5 μg of dynamin (shown for PS monolayers in Figure 1A), and this saturating amount was used throughout the experiments. The membrane activity of dynamin was studied in single-lipid (Figure 1B) and in mixed-lipid systems (see below), and large differences were observed when the composition of the lipid monolayer was varied.

Lipid Specificity of Membrane Activity. Immediately after injecting dynamin into the subphase, the surface pressure of the monolayer started to rise and reached equilibrium after 30−45 min. The kinetics and extent of the surface pressure increase were very sensitive to the composition of the lipid monolayer (Figure 1B). To determine the lipid specificity of dynamin insertion, the composition of the lipid monolayer was varied systematically, and the surface pressure increase was measured after reaching equilibrium (Figure 2). For optimal sensitivity, lipid monolayers were used at an initial surface pressure of 25 mN/m (see below). With respect to single-lipid monolayers (Figure 2A), insertion was maximal into PA monolayers, but considerable insertion was also found for PS and the phosphoinositides: phosphatidylinositol 4-phosphate (PtdIns-4-P) and phosphatidylinositol 4,5-bis-phosphate (PtdIns-4,5-P$_2$). There was hardly any insertion into overall neutral phosphatidylcholine (PC) and phosphatidylethanolamine (PE) monolayers. Similar results were obtained using physiologically relevant mixed-lipid monolayers composed of PC, PE, PS, and cholesterol (Chol) in a 1:1:1:1 mole ratio to which 20 mol % of an additional lipid (as indicated) was added (*26*). In these mixed-lipid monolayers (Figure 2B), dynamin only inserted efficiently when PA, PtdIns-4-P, or PtdIns-4,5-P$_2$ was present. Note that apart from the control which did not contain anionic lipids, all mixed-lipid monolayers contained 20 mol % of PS. Moreover, dynamin did not insert efficiently in mixed-lipid monolayers containing as an anionic lipid, only PS.

The penetrative power of dynamin was determined as a function of the initial surface pressure of the lipid monolayer, i.e., the surface pressure before injecting dynamin. Higher initial surface pressures of the monolayer correlate with higher packing densities of the lipids, and hinder protein insertion. As a result, the dynamin-induced surface pressure increase is progressively reduced (Figure 3). Extrapolation of these data yields the exclusion pressure, defined as the surface pressure beyond which dynamin cannot insert. The results on single-lipid monolayers (Figure 3A) indicated that dynamin cannot penetrate zwitterionic (PC) monolayers at high initial surface pressures of the lipid monolayer, and the exclusion pressure for PC was 28.7 mN/m. In contrast, dynamin inserted into PS and PA lipid monolayers up to much higher surface pressures: exclusion pressures of 34.5 and 58.3 mN/m were found, respectively. The latter (theoretical) value is considerably higher than the collapse pressure of the lipid monolayer (about 45 mN/m, not shown), and indicates that dynamin is able to insert even at initial surface pressures by far exceeding the "physiological range" of 30−35 mN/m (see Discussion). The surface pressure dependence of insertion of dynamin into mixed-lipid monolayers was
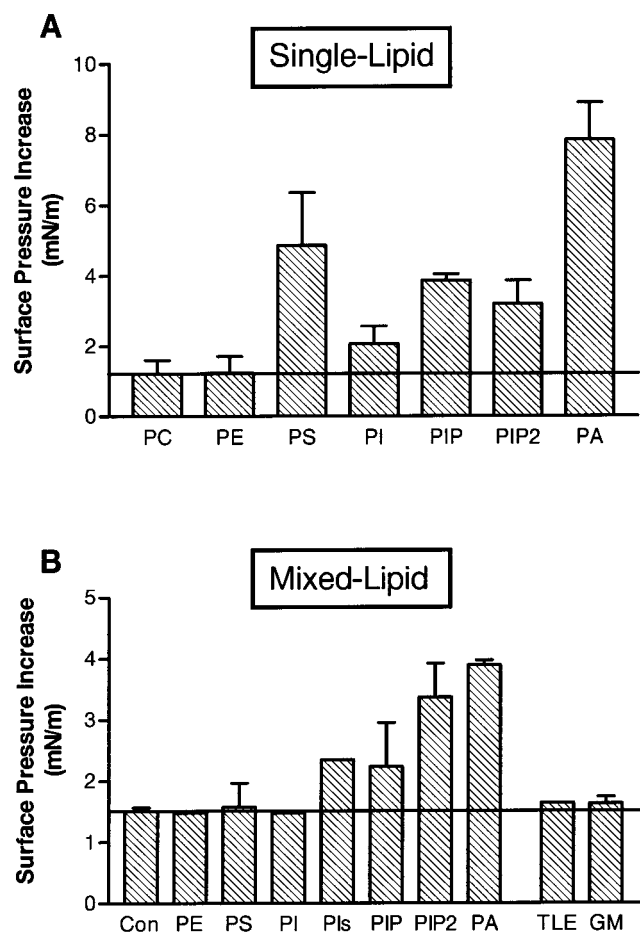
FIGURE 2: Lipid dependency of membrane activity. Dynamin (2.5 μg) was injected underneath a lipid monolayer, and the increase in surface pressure was determined at equilibrium. (A) Single-lipid monolayers. (B) Mixed-lipid monolayers of PC/PE/Chol/PS 1:1:1:1 with an additional 20 mol % of the indicated lipid (PE, PS, PI, PIs, PIP, PIP2, PA); PIs, brain lipid extract enriched in PtdIns-4-P and PtdIns-4,5-P$_2$; Con (control), PC/PE/Chol 1:1:1; TLE, a representative brain lipid extract containing ~20 mol % anionic phospholipids (type VII) to which no lipids were added; GM, galactosylceramide-containing lipid mixture with 10 mol % PtdIns-4,5-P$_2$ (*12*). Horizontal lines (A, B) indicate insertion in the absence of anionic lipids. Standard deviation as indicated (3−5 determinations); for experimental conditions, see legend to Figure 1.

also determined (Figure 3B and Table 1), and exclusion pressures were ~30, 34, and 37 mN/m for the mixed-lipid monolayers containing PtdIns-4-P, PtdIns-4,5-P$_2$, and PA, respectively. These data show that dynamin is capable of inserting into lipid monolayers spread at physiological surface pressures as long as they contain PtdIns-4,5-P$_2$ or PA, and that insertion is most pronounced in the presence of PA.
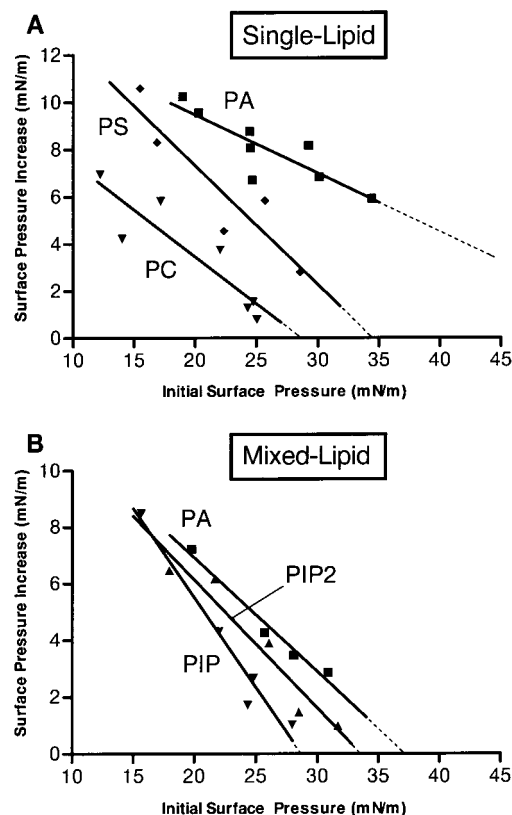

FIGURE 3: Surface pressure dependence of membrane activity. The monolayer surface pressure increase as a function of the initial surface pressure. (A) Single-lipid monolayers. (B) Mixed-lipid monolayers. Constant area experiments at 37 °C; curves determined by linear regression analysis; the intercept with the *x*-axis defines the monolayer exclusion pressure; for the mixed-lipid monolayer containing PA, an independent batch of dynamin was used (see Table 1).

Lipid Dependency of Binding. To quantify the amount of dynamin stably interacting with the lipid monolayer, the protein was ^{14}C-labeled using the method of Dottavio-Martin and Ravel (*22*) which is performed at neutral pH and does not change the charge of the amino groups. On average, ~9 amino groups were labeled per dynamin monomer (864 amino acids); the efficiency and lipid specificity of dynamin insertion into lipid monolayers were not affected (not shown). Figure 4A shows the simultaneous recording of surface pressure and surface radioactivity after injecting ^{14}C-labeled dynamin underneath a mixed-lipid monolayer containing PtdIns-4,5-P$_2$. Directly following injection of dynamin, the radiolabeled protein associated with and inserted into the lipid monolayer. Washing did not affect surface pressure and only reduced surface radioactivity by ~8%, showing that dynamin

Table 1: Exclusion Pressures and Estimated Molecular Areas of Dynamin Insertion into Mixed-Lipid Monolayers[a]

| | | | estimated molecular area of dynamin insertion (nm^2 per monomer)[d] | | |
| | exclusion pressure (mN/m)[b] | | initial surface pressure | | |
mixed-lipid monolayer containing	dynamin batch-1[c]	dynamin batch-2	25 mN/m	30 mN/m	35 mN/m
PtdIns-4-P	28.7	32.0	55 ± 13	~0	0
PtdIns-4,5-P$_2$	33.6	34.9	53 ± 2	29 ± 6	0
PA	ND	37.2	102 ± 4	75	26

[a] Constant area experiments (see legend to Figure 1). [b] The exclusion pressure was determined by linear regression analysis (see Figure 3). [c] The results with two independent batches of dynamin are shown; ND, not determined. [d] The molecular area of dynamin insertion was calculated from the binding data obtained at 25 mN/m (Figure 4B; assuming identical binding at initial surface pressures of 25−35 mN/m), the average surface pressure increase induced by dynamin (Figures 2B and 3B), and the compression curves of the lipid monolayers (see text).
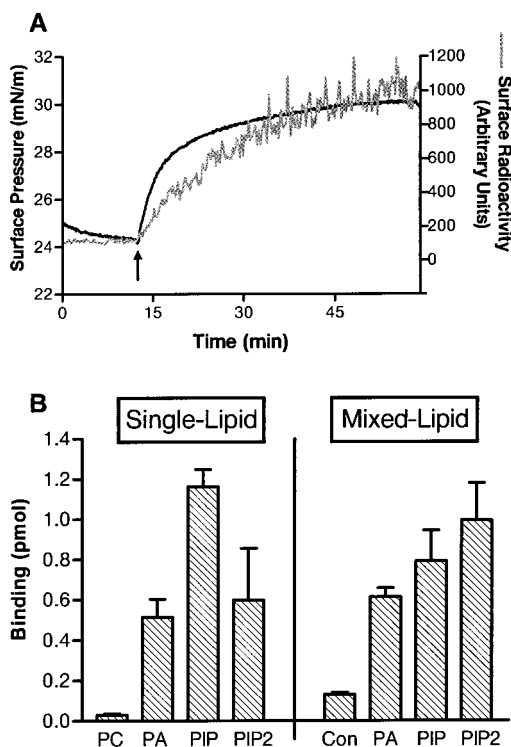
FIGURE 4: Lipid dependency of binding. (A) Binding and insertion of ^{14}C-labeled dynamin (23.5 μg, 235 pmol) injected (arrow) into the subphase (19 mL) underneath a mixed-lipid monolayer with PtdIns-4,5-P$_2$ followed on-line. At $t = 60$ min, the monolayer was subjected to a washing procedure and the surface radioactivity determined (see text). The collected monolayer contained 14.6 pmol of dynamin (monolayer area of 30.2 cm^2). In (B), ^{14}C-labeled dynamin (2.5 μg) was injected into the subphase (1.6 mL), and after the surface pressure reached equilibrium, the monolayer was washed and collected. The monolayer radioactivity was used to calculate the amount of dynamin stably bound to the lipid monolayer (monolayer area of 3.14 cm^2). Constant area experiments; initial surface pressure of the lipid monolayer, 25 mN/m (37 °C); standard deviation as indicated (3−7 determinations).

deeply inserted into the acyl chain region of the lipid layer and that, once inserted, dynamin interaction with the monolayer was stable on the time-scale of the experiment (not shown).

To determine the lipid specificity of dynamin−lipid binding, ^{14}C-labeled dynamin was allowed to insert into various lipid monolayers, and after the surface pressure reached equilibrium, the subphase was refreshed repeatedly to remove loosely bound dynamin. The monolayers were collected, and their radioactivity was determined; results are shown in Figure 4B. There was hardly any dynamin binding to neutral lipid monolayers composed of PC or an equimolar mixture of PC, PE, and Chol. In contrast, between 0.5 and 1.2 pmol of dynamin, 2−5% of the injected amount, interacted with single- and mixed-lipid monolayers containing phosphoinositides or PA. Several in vitro studies indicate that PtdIns-4,5-P$_2$ is the preferred binding partner of dynamin's PH domain, although it is quite promiscuous in its phospholipid binding when compared to other PH domains (*21, 27, 28*). In line with these observations, dynamin bound slightly more efficiently to mixed-lipid monolayers containing PtdIns-4,5-P$_2$ than to those containing PtdIns-4-P or PA (Figure 4B). In single-lipid monolayers, binding was more efficient to PtdIns-4-P, suggesting that there is a charge density optimum for dynamin−anionic lipid interaction,
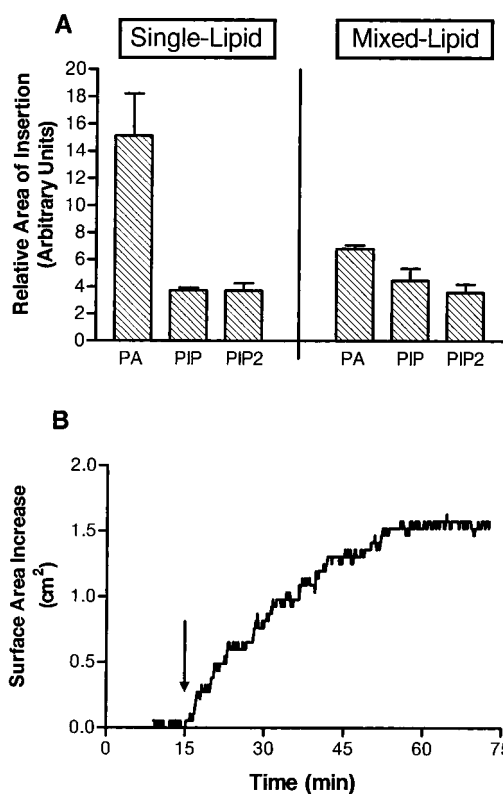

FIGURE 5: Relative area of insertion. (A) The surface pressure increase, normalized to the amount of dynamin bound, is a direct measure of the relative area of insertion of dynamin. Binding and insertion were determined on the same monolayer using ^{14}C-labeled dynamin. Constant area experiment; initial surface pressure of the lipid monolayer, 25 mN/m (37 °C); standard deviation as indicated (3−7 determinations). In (B) dynamin (17 μg) was injected (arrow) into the subphase (10 mL) underneath a mixed-lipid monolayer with PtdIns-4,5-P$_2$. The surface pressure was kept constant at 30 mN/m using a computer-controlled moveable barrier, and the surface area increase of the monolayer was followed in time (20 °C). The initial surface area of the lipid monolayer was 19.35 cm^2; a typical experiment is shown.

which is exceeded in pure PtdIns-4,5-P$_2$ monolayers (see *29*). Assuming an area of contact with the lipid monolayer of 200−400 nm^2 for a dynamin homotetramer with dimensions of 10 by 20−40 nm (*9*), binding of 1 pmol of dynamin (monomer) would cover 10−20% of the area of the lipid monolayer, with a lipid-to-dynamin monomer mole ratio of ∼800. A remarkable finding was that among the anionic lipids tested, dynamin bound the least efficiently to monolayers containing PA, while the surface pressure increase measured in these PA-containing monolayers was the greatest (Figure 2; identical results were obtained using ^{14}C-labeled dynamin; see below). Apparently, in the presence of PA, a larger part of dynamin inserted into the monolayer.

Relative Area of Insertion. The penetrative power of dynamin is determined by the number of dynamin molecules binding to the lipid monolayer as well as by the molecular area of the part of dynamin inserting into the lipid layer. Because the shapes of the compression curves of the lipid monolayers used are almost identical (not shown; see *30, 31*), the surface pressure increase normalized to the amount of dynamin bound can be used as a direct measure of the relative area of insertion of dynamin (Figure 5A). The results show that although there were clear differences in the binding efficiency to monolayers containing PtdIns-4-P and those

containing PtdIns-4,5-P$_2$ (see Figure 4B), the area of dynamin inserting into these monolayers was virtually identical. On the other hand, the presence of PA in the monolayer resulted in a dramatic increase in the area of insertion. Comparing PA with the phosphoinositides in single-lipid monolayers, the area of dynamin insertion was 4-fold greater for PA, while the presence of PA in mixed-lipid monolayers resulted in a 1.5−1.9-fold increase in the area of insertion (using monolayers spread at 25 mN/m).

An estimate of the actual molecular area of insertion can be made based on the surface pressure increase induced by dynamin at constant monolayer surface area, and the pressure−area curve of the lipid monolayer, assuming the molecular area of the lipids is not affected by interacting with dynamin (see *32*, *33*). The results (Table 1) indicated that, as long as PtdIns-4,5-P$_2$ or PA were present, a substantial part of dynamin inserted into the mixed-lipid monolayers, even at surface pressures exceeding 30 mN/m. The molecular area of dynamin insertion was also measured directly as the increase in monolayer surface area necessary to maintain a constant surface pressure during dynamin insertion (Figure 5B). The average molecular area of the part of dynamin that inserted into a mixed-lipid monolayer in the presence of PtdIns-4,5-P$_2$, at 30 mN/m, was 31 ± 6 nm^2 per monomer, very similar to the value obtained at constant surface area (see Table 1). Collectively, these data showed that the molecular area of the part of dynamin penetrating the lipid layer strongly depended on lipid composition, being greatest in the presence of PA.

Molecular Dissection of Membrane Activity. To determine which part of the dynamin molecule is responsible for the binding to anionic lipids, and which part is actually penetrating the lipid layer, the membrane activity of dynamin was compared to that of truncated dynamin (ΔPRD) lacking the proline- and arginine-rich C-terminal 100 amino acids, and of the isolated PH domain of dynamin. No difference was observed in membrane activity toward PtdIns-4,5-P$_2$ containing mixed-lipid monolayers between dynamin and the ΔPRD mutant (surface pressure increase of 4.1 ± 0.1 and 4.5 ± 0.2 mN/m for dynamin and ΔPRD, respectively; $n = 3$, initial surface pressure of 25 mN/m), strongly suggesting that the PRD is not involved in binding or in insertion. The results obtained using the isolated PH domain of dynamin were nonconclusive. Added at equimolar amounts as compared to full-length dynamin, the isolated PH domain did not induce any surface pressure increase, but we were also unable to detect binding to the PtdIns-4,5-P$_2$-containing mixed-lipid monolayers using the ^{14}C-labeled PH domain of dynamin-1 and both on-line and off-line binding experiments (not shown; cf. Figure 4). Thus, the low membrane activity observed for dynamin's PH domain is probably due to the extremely low affinity of the isolated monomeric PH domain of dynamin for anionic lipids such as phosphoinositides (*21*), and does not exclude the possibility that the PH domain in the context of full-length dynamin inserts into the lipid monolayer.

To examine the importance of the PH domain in the context of full-length dynamin, the influence of various isolated PH domains on the membrane activity of dynamin was determined (Figure 6; for a review on the structure and function of PH domains, see *34*). The isolated PH domain of phospholipase Cδ (PLCδ-PH) was used because it has a
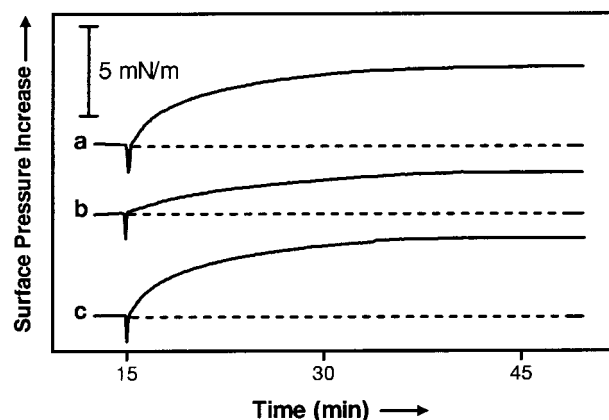

FIGURE 6: Role of the PH domain in membrane activity. Dynamin (25 pmol) was injected without (a) or with preincubation of the PtdIns-4,5-P$_2$ mixed-lipid monolayer for 15 min with (b) the isolated PH domain of PLC-δ (25 pmol), or (c) the mutated PH domain of PLC-δ defective in phosphoinositide binding (50 pmol). Only the wild-type PH domain of PLC-δ blocks PtdIns-4,5-P$_2$ binding sites and reduced the membrane activity of dynamin. Typical experiments are shown. Constant area experiments; initial surface pressure of the lipid monolayer, 25 mN/m (37 °C).

very high affinity for PtdIns-4,5-P$_2$ (*19*, *35*) and was shown to inhibit coated vesicle formation in a cell-free system reconstituting clathrin-mediated endocytosis (*36*). Preincubating the monolayer with PLCδ-PH reduced the membrane activity of an equimolar amount of dynamin by 49% (Figure 6), and a further reduction, to 35% of the control, was found after preincubation with a 2-fold molar excess of PLCδ-PH (not shown). To check whether the inhibition by PLCδ-PH was the result of high-affinity binding to PtdIns-4,5-P$_2$ present in the monolayer, a point-mutated PLCδ-PH defective in phosphoinositide binding was used (*36*). Preincubating the monolayer with the mutated PLCδ-PH had no effect on the membrane activity of dynamin. These data suggest that wild-type PLCδ-PH prevents interaction of dynamin with the monolayer by blocking the PtdIns-4,5-P$_2$ binding sites. Apparently, the membrane activity of dynamin critically depends on binding to anionic lipids such as PtdIns-4,5-P$_2$, which, based on extensive literature data (*16*, *17*, *37*), most likely occurs via the PH domain of dynamin.

Because the GTPase activity of dynamin plays a central role in its biological activity, the influence of nucleotides on the membrane activity of dynamin was studied extensively using up to 1 mM GTP or up to 0.5 mM GTPγS, added before or after dynamin. In these experiments, performed using monolayers of various lipid compositions, the membrane activity of dynamin was not affected (results not shown), indicating that membrane activity and GTPase activity were not related.

DISCUSSION

Dynamin Is a Membrane-Active Molecule. The most important result of the current study is that dynamin is a membrane-active molecule capable of penetrating into the acyl chain region of membrane lipids. The penetrative power of dynamin is remarkably lipid-dependent, and strongly enhanced by PtdIns-4,5-P$_2$ and in particular by PA. Data were collected using as a model system lipid monolayers spread at the air−water interface. In several studies, the properties of membrane-active proteins and peptides have been studied

using both bilayer membranes and lipid monolayers, and an excellent correspondence was observed between (bio)-membrane systems, on one hand, and monolayers at a surface pressure of 30−35 mN/m, on the other hand (reviewed in *14*, *15*). Thus, when used at sufficiently high surface pressures, lipid monolayers are a reliable model system to study the mechanism by which a membrane-active protein such as dynamin inserts into the plasma membrane. Consequently, the pronounced membrane activity of dynamin and its strong lipid dependence are expected to have important implications for the biological activity of dynamin in vivo.

In view of the fact that many biomembranes, including the plasma membrane, appear to contain microdomains relatively enriched in particular lipids and proteins (*38*), dynamin−lipid interaction was characterized using both single-lipid and mixed-lipid systems. In both cases, the membrane activity of dynamin depends on electrostatic interactions, and efficient binding and insertion is only observed in the presence of anionic phospholipids. The lipid dependency of binding to mixed-lipid monolayers together with extensive literature data on the role of dynamin's PH domain in membrane binding (*16*, *17*, *21*) strongly suggest that dynamin binds to the lipid monolayer via its PH domain. Indeed, blocking the PtdIns-4,5-P$_2$ binding sites of a mixed-lipid monolayer strongly reduces the membrane activity of dynamin (Figure 6). Experiments with a deletion mutant of dynamin show that the PRD of dynamin is not involved in binding to lipid monolayers (see Results) or liposomes (*7*, *39*). Thus, the mode of dynamin−lipid binding is the same in monolayer and bilayer systems. The PH domain appears to be responsible for protein−lipid interactions, whereas the role of the PRD is to interact with accessory proteins, in particular those containing SH3 binding sites (*7*, *16*, *39*, *40*).

At physiological lipid packing densities, dynamin only inserts into single-lipid monolayers of PS and PA, and into mixed-lipid monolayers containing either PtdIns-4,5-P$_2$ or PA. At even higher lipid packing densities (surface pressure ≥35 mN/m), dynamin insertion is restricted to PA-containing lipid systems (Table 1). The results obtained with mixed-lipid monolayers can be directly compared to those obtained by Takei et al. (*26*) using liposomes of the same lipid composition and studying the formation of dynamin-coated tubules upon interaction with brain cytosol. Tubulation was most efficient in the presence of PA, much less efficient with phosphoinositides, and the least efficient with PS- and PE-containing liposomes. Thus, the membrane activity of dynamin and the capacity to tubulate liposomes closely match, suggesting that insertion of dynamin into the membrane is of crucial importance for functional dynamin−membrane interaction. Dynamin undergoes a conformational change upon GTP hydrolysis inducing vesiculation of dynamin-decorated lipid tubules in vitro (*7*, *11*). However, GTP does not alter the ability of purified dynamin to bind lipid or tubulate liposomes (*7*, *26*). In line with these findings, the membrane activity of dynamin is not affected by adding GTP or a nonhydrolyzable analogue, indicating that membrane activity and GTPase activity are not related. The capacity of dynamin to insert into membranes is strongly lipid-dependent but not influenced by the conformational change in dynamin upon GTP hydrolysis.

The molecular area of the part of dynamin inserting into the lipid monolayer strongly depends on lipid composition and packing. At physiological lipid packing densities, the molecular area of insertion into mixed-lipid monolayers is increased more than 2-fold in the presence of PA as compared to that in the presence of PtdIns-4,5-P$_2$ (Table 1). Estimates of the molecular area of insertion indicate that under these conditions a large part of dynamin, 26−75 nm^2 per monomer, inserts into the lipid layer. Comparing these values to the dimensions of dynamin, 10 by 20−40 nm for an isolated tetrameric dynamin (*9*) and 10 nm by 13 nm for a lipid-bound dimer (*41*), shows that most of the contact area between dynamin and the lipid interface must be involved in this interaction. The membrane activity of dynamin at high lipid packing densities and the large area of insertion are quite remarkable. For example, the membrane activity of influenza hemagglutinin (HA), the protein responsible for virus−membrane fusion and the best characterized fusogenic protein to date, is negligible at pressures exceeding 30 mN/m; the area of insertion of the part of HA inserting into the lipid layer, the N-terminal fusion peptide, is too small to allow detection (*42*).

Which part of dynamin is responsible for membrane activity? In agreement with data on dynamin−membrane binding in vitro (*7*, *39*), deleting dynamin's PRD had no effect on membrane activity, indicating that it is not responsible for lipid insertion. We were unable to prove or disprove lipid insertion of dynamin's PH domain in the context of full-length dynamin (see Results); however, based on the large molecular area of the inserted part of dynamin and the relatively small size of the PH domain, we consider it unlikely that the PH domain is solely responsible for dynamin's membrane activity; i.e., other parts of dynamin are likely to insert instead of, or in addition to, the PH domain. The PH domain may mediate lipid binding and the proper positioning of dynamin in order to allow insertion of another, and as yet unidentified, domain of dynamin into the membrane [cf. the 'tether and fix' model proposed for PLC-δ (*43*)]. This hypothesis is supported by the fact that the dynamin-like proteins, vps1p and dnm1p, lack both the PRD and PH domains, yet, like dynamin, seem to regulate membrane fission (*44*).

Lipid Metabolism and Dynamin Function: A New Model. Receptor-mediated endocytosis depends on binding of clathrin and adaptor protein-2 to the plasma membrane, and is regulated by dynamin and a large number of additional accessory proteins such as amphiphysin and endophilin (*1*). Amphiphysin and endophilin bind not only to dynamin, but also to the PRD of synaptojanin, a protein that co-localizes with dynamin in nerve terminals (*45*, *46*). Thus, the endocytic machinery contains at least two essential lipid-modifying enzymes, endophilin I and synaptojanin. Synaptojanin is an inositol-5-phosphatase converting PtdIns-4,5-P$_2$ into PtdIns-4-P (*45*). Endophilin I is a lyso-PA (LPA) acyltransferase capable of converting, in vitro, LPA (1-oleoyl) into PA using oleoyl- or arachidonoyl-CoA as the acyl donor. This lipid-transfer reaction was shown to be required for the formation of synaptic-like microvesicles in perforated cells (*18*), while microinjecting nerve terminals with antibodies against endophilin blocked synaptic vesicle recycling, and removing endophilin from the cytosol strongly inhibited dynamin-coated tubule formation of synaptic membranes (*47*).

What could be the role of local lipid metabolism in dynamin-dependent endocytosis? Although a detailed model

explaining the involvement of particular lipids in membrane bending and fission during endocytosis is still premature, the pronounced membrane activity of dynamin is likely to be important. Dynamin binds more efficiently to PtdIns-4,5-P_2 but inserts much more extensively into PA-containing lipid systems. Thus, high concentrations of PtdIns-4,5-P_2 in the neck region of a deeply invaginated coated pit would be expected to result in very efficient binding of dynamin via its PH domain, while the local generation of PA by dynamin-bound endophilin induces deep penetration of dynamin into the membrane. In this *lipid-activated fission model* of dynamin-mediated endocytosis, an oligomer of deeply inserted dynamin destabilizes the membrane and induces membrane fission. In an alternative model (*18*), dynamin-bound endophilin I is proposed to induce membrane constriction and fission by inducing negative membrane curvature, the result of the conversion of inverted-cone-shaped LPA into cone-shaped PA. We consider this model, in its simple form, less likely because at the neutral pH of the cytosol, even unsaturated (dioleoyl) PA behaves as a cylindrical, bilayer-preferring, lipid [(*48*, *49*); K. N. J. Burger, V. Chupin, and B. de Kruijff, unpublished results; also see (*50*)]. It is important to note that dynamin may control membrane morphogenesis throughout the coated vesicle formation process (*51*). Disruption of endophilin function in stimulated synapses has been shown to block invagination of clathrin-coated pits (*47*). If dynamin inserts only into the cytoplasmic leaflet of the membrane, this would create a large asymmetry in surface area between the two membrane leaflets, which could dramatically affect membrane curvature. In fact, insertion of dynamin into the outer leaflet of liposomes could be the driving force for their conversion into very narrow tubules (30 nm in diameter for the lipid part; see *7*). The liposomes have equally sized membrane leaflets, while the surface area of the outer membrane leaflet of the dynamin-coated tubules is ~50% greater than that of the inner leaflet. Thus, together with endophilin, dynamin may also act at earlier stages of endocytosis, inducing membrane curvature as coated pits become more invaginated. In contrast to endophilin, synaptojanin could play a role in endocytosis as a negative regulator of the membrane activity of dynamin; a conversion of PtdIns-4,5-P_2 into PtdIns-4-P should reduce both membrane binding and insertion of dynamin.

Model Comparison. Two main models have been proposed for the role of dynamin in the actual membrane fission event: the pinchase-model and the molecular switch model (see the introduction). In the first model, dynamin is thought to be directly responsible for membrane fission, and fission is coupled to GTP hydrolysis. In the second model, GTP-bound dynamin activates downstream effectors and is itself not directly responsible for membrane fission. The lipid-activated fission model combines elements of both the pinchase and the molecular switch model, and is in good agreement with both in vitro and in vivo data on dynamin-dependent endocytosis. Membrane fission is energetically unfavorable, and can only be envisaged when local defects destabilize the lipid packing of the membrane (*50*, *52*, *53*). In vitro data provide strong evidence for the capacity of dynamin to destabilize membranes. When lipid systems are used that allow insertion of dynamin into the membrane, for example, pure PS (*7*) or a brain lipid extract mainly composed of PS [Folch fraction I; (*11*)], membrane tubules are formed which are destabilized by the conformational change in the dynamin ring upon GTP hydrolysis (*7*). Vesiculation is not observed using preformed lipid nanotubes composed of non-hydroxy fatty-acid galactosylceramide, PC, Chol, and PtdIns-4,5-P_2 [in a 4:4:1:1 molar ratio (*12*)], a lipid mixture that does not favor dynamin insertion (Figure 2B). Together, these in vitro data suggest a relation between the membrane activity of dynamin, which is very sensitive to membrane lipid composition, and the capacity of dynamin to induce membrane fission. Importantly, in vivo data indicate that membrane fission during endocytosis does not depend on dynamin's maximal stimulated rate of GTP hydrolysis (*13*). We propose that the local formation of PA is the trigger for dynamin-mediated membrane fission, and that assembly-stimulated GTP hydrolysis by dynamin is required to switch dynamin off and release the fission machinery into the cytosol. In contrast to the assembly-stimulated GTPase activity, basal GTPase activity or GTP binding is required for coated vesicle formation (*5*, *6*) probably because dynamin−GTP activates accessory proteins such as endophilin which are essential in coated vesicle formation. Finally, it is important to note that dynamin self-assembly does not appear to be a prerequisite for efficient endocytosis, given the fact that transferrin uptake is enhanced in cells overexpressing a dynamin mutant with a defect in self-assembly measured in vitro (*13*). Thus, not dynamin collars, but smaller supramolecular aggregates of dynamin may turn out to be the functional dynamin unit in vivo.

CONCLUDING REMARKS

It was shown earlier that dynamin's GTPase activity is not directly involved in the induction of membrane fission in vivo, but instead used to regulate downstream effectors of membrane fission (*13*). Our data now indicate that one of the downstream effectors is likely to be dynamin itself. Dynamin is a membrane-active molecule capable of penetrating into the acyl chain region of membrane lipids. Dynamin's penetrative power is greatly enhanced by PA but not nucleotide-dependent. Not GTP hydrolysis but local lipid metabolism is expected to activate dynamin. Endophilin, a dynamin-binding partner, is likely to be a key player. The endophilin-mediated formation of PA could trigger insertion of dynamin into the membrane and induce membrane bending and/or fission. Interestingly, a completely unrelated protein but also converting LPA into PA was found to be essential in a membrane fission reaction in the Golgi complex (*54*). PA is unique among anionic lipids because of its small and highly charged headgroup very close to the glycerol backbone. The local generation of PA followed by the insertion of a membrane-active protein capable of bending or destabilizing the membrane may thus turn out to be a general theme in intracellular membrane fission events.

REFERENCES

1. Schmid, S. L., McNiven, M. A., and De Camilli, P. (1998) *Curr. Opin. Cell Biol. 10*, 504−512.
2. Poodry, C. A., and Edgar, L. (1979) *J. Cell Biol. 81*, 520−527.
3. Kosaka, T., and Ikeda, K. (1983) *J. Neurobiol. 14*, 207−225.
4. Takei, K., McPherson, P. S., Schmid, S. L., and De Camilli, P. (1995) *Nature 374*, 186−190.

5. Herskovits, J. S., Burgess, C. C., Obar, R. A., and Vallee, R. B. (1993) *J. Cell Biol. 122*, 565−578.

6. Damke, H., Baba, T., Warnock, D. E., and Schmid, S. L. (1994) *J. Cell Biol. 127*, 915−934.

7. Sweitzer, S. M., and Hinshaw, J. E. (1998) *Cell 93*, 1021−1029.

8. Muhlberg, A. B., Warnock, D. E., and Schmid, S. L. (1997) *EMBO J. 16*, 6676−6683.

9. Hinshaw, J. E., and Schmid, S. L. (1995) *Nature 374*, 190−192.

10. Warnock, D. E., Hinshaw, J. E., and Schmid, S. L. (1996) *J. Biol. Chem. 271*, 22310−22314.

11. Takei, K., Slepnev, V. I., Haucke, V., and De Camilli, P. (1999) *Nat. Cell Biol. 1*, 33−39.

12. Stowell, M. H. B., Marks, B., Wigge, P., and McMahon, H. T. (1999) *Nat. Cell Biol. 1*, 27−32.

13. Sever, S., Muhlberg, A. B., and Schmid, S. L. (1999) *Nature 398*, 481−486.

14. Demel, R. A. (1994) *Subcell. Biochem. 23*, 83−120.

15. Marsh, D. (1996) *Biochim. Biophys. Acta 1286*, 183−223.

16. Achiriloaie, M., Barylko, B., and Albanesi, J. P. (1999) *Mol. Cell. Biol. 19*, 1410−1415.

17. Vallis, Y., Wigge, P., Marks, B., Evans, P. R., and McMahon, H. T. (1999) *Curr. Biol. 9*, 257−260.

18. Schmidt, A., Wolde, M., Thiele, C., Fest, W., Kratzin, H., Podtelejnikov, A. V., Witke, W., Huttner, W. B., and Söling, H. D. (1999) *Nature 401*, 133−141.

19. Lemmon, M. A., Ferguson, K. M., O'Brien, R., Sigler, P. B., and Schlessinger, J. (1995) *Proc. Natl. Acad. Sci. U.S.A. 92*, 10472−10476.

20. Ferguson, K. M., Lemmon, M. A., Schlessinger, J., and Sigler, P. B. (1995) *Cell 83*, 1037−1046.

21. Klein, D. E., Lee, A., Frank, D. W., Marks, M. S., and Lemmon, M. A. (1998) *J. Biol. Chem. 273*, 27725−27733.

22. Dottavio-Martin, D., and Ravel, J. M. (1978) *Anal. Biochem. 87*, 562−565.

23. Bradford, M. M. (1976) *Anal. Biochem. 72*, 248−254.

24. Rouser, G., Fleischer, S., and Yamamoto, A. (1970) *Lipids 5*, 494−496.

25. Demel, R. A. (1982) in *Membranes and Transport* (Martonosi, A. N., Ed.) Vol. 1, pp 159−164, Plenum Press, New York.

26. Takei, K., Haucke, V., Slepnev, V., Farsad, K., Salazar, M., Chen, H., and De Camilli, P. (1998) *Cell 94*, 131−141.

27. Kavran, J. M., Klein, D. E., Lee, A., Falasca, M., Isakoff, S. J., Skolnik, E. Y., and Lemmon, M. A. (1998) *J. Biol. Chem. 273*, 30497−30508.

28. Barylko, B., Binns, D., Lin, K. M., Atkinson, M. A., Jameson, D. M., Yin, H. L., and Albanesi, J. P. (1998) *J. Biol. Chem. 273*, 3791−3797.

29. James, S. R., Paterson, A., Harden, T. K., Demel, R. A., and Downes, C. P. (1997) *Biochemistry 36*, 848−855.

30. James, S. R., Demel, R. A., and Downes, C. P. (1994) *Biochem. J. 298*, 499−506.

31. Demel, R. A., Yin, C. C., Lin, B. Z., and Hauser, H. (1992) *Chem. Phys. Lipids 60*, 209−223.

32. Batenburg, A. M., Demel, R. A., Verkleij, A. J., and de Kruijff, B. (1988) *Biochemistry 27*, 5678−5685.

33. Török, Z., Demel, R. A., Leenhouts, J. M., and de Kruijff, B. (1994) *Biochemistry 33*, 5589−5594.

34. Blomberg, N., Baraldi, E., Nilges, M., and Saraste, M. (1999) *Trends Biochem. Sci. 24*, 441−445.

35. Raucher, D., Stauffer, T., Chen, W., Shen, K., Guo, S., York, J. D., Sheetz, M. P., and Meyer, T. (2000) *Cell 100*, 221−228.

36. Jost, M., Simpson, F., Kavran, J. M., Lemmon, M. A., and Schmid, S. L. (1998) *Curr. Biol. 8*, 1399−1402.

37. Lee, A., Frank, D. W., Marks, M. S., and Lemmon, M. A. (1999) *Curr. Biol. 9*, 261−264.

38. Brown, D. A., and London, E. (1998) *Annu. Rev. Cell Dev. Biol. 14*, 111−136.

39. Lin, H. C., Barylko, B., Achiriloaie, M., and Albanesi, J. P. (1997) *J. Biol. Chem. 272*, 25999−26004.

40. Simpson, F., Hussain, N. K., Qualmann, B., Kelly, R. B., Kay, B. K., McPherson, P. S., and Schmid, S. L. (1999) *Nat. Cell Biol. 1*, 119−124.

41. Hinshaw, J. E. (1999) *Curr. Opin. Struct. Biol. 9*, 260−267.

42. Burger, K. N. J., Wharton, S. A., Demel, R. A., and Verkleij, A. J. (1991) *Biochemistry 30*, 11173−11180.

43. Essen, L. O., Perisic, O., Cheung, R., Katan, M., and Williams, R. L. (1996) *Nature 380*, 595−602.

44. Van der Bliek, A. M. (1999) *Trends Cell Biol. 9*, 96−102.

45. McPherson, P. S., Garcia, E. P., Slepnev, V. I., David, C., Zhang, X., Grabs, D., Sossin, W. S., Bauerfeind, R., Nemoto, Y., and De Camilli, P. (1996) *Nature 379*, 353−357.

46. Ringstad, N., Nemoto, Y., and De Camilli, P. (1997) *Proc. Natl. Acad. Sci. U.S.A. 94*, 8569−8574.

47. Ringstad, N., Gad, H., Löw, P., Di Paolo, G., Brodin, L., Shupliakov, O., and De Camilli, P. (1999) *Neuron 24*, 143−154.

48. Verkleij, A. J., de Maagd, R., Leunissen Bijvelt, J., and de Kruijff, B. (1982) *Biochim. Biophys. Acta 684*, 255−262.

49. Farren, S. B., Hope, M. J., and Cullis, P. R. (1983) *Biochem. Biophys. Res. Commun. 111*, 675−682.

50. Burger, K. N. J. (2000) *Traffic 1*, 605−613.

51. Roos, J., and Kelly, R. B. (1997) *Trends Cell Biol. 7*, 257−259.

52. Burger, K. N. J. (1998) *Curr. Top. Membr. 44*, 403−445.

53. Jahn, R., and Südhof, T. C. (1999) *Annu. Rev. Biochem. 68*, 863−911.

54. Weigert, R., Silletta, M. G., Spano, S., Turacchio, G., Cericola, C., Colanzi, A., Senatore, S., Mancini, R., Polishchuk, E. V., Salmona, M., Facchiano, F., Burger, K. N. J., Mironov, A., Luini, A., and Corda, D. (1999) *Nature 402*, 429−433.